Measuring the interference between the short- and long-distance contributions in $B^+ \to K^+\mu^+\mu^-$ decays with Run2 data

LHCb-UK 2020

Lakshan[1], Kostas[1], Patrick[2], Oliver[2], Tom[3] and Ulrik[4]

06-01-2020

[1]University of Bristol
[2]University of Zurich
[3]University of Warwick
[4]Monash University

$b \to sll$ transitions to probe New Physics

NP searches using observables that,

- Have a small SM contribution,
- Can be measured to a high precision,
- Can be predicted to a high precision.

b → sll transitions to probe New Physics

NP searches using observables that,

- Have a small SM contribution,
- Can be measured to a high precision,
- Can be predicted to a high precision.

Flavour Changing Neutral Currents in SM

- GIM suppressed
- Loop level
- Left-handed chirality

NP can easily violate the above.

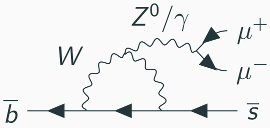

lakshan.ram@cern.ch

Effective Field Theory Formalism

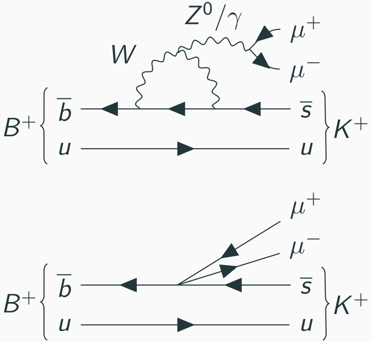

- In the Effective Field Theory (EFT), the heavy physics ($> \mathrm{M}_W$) is integrated out.
- The Wilson coefficients contain all information about short-distance physics.

Effective Field Theory Formalism

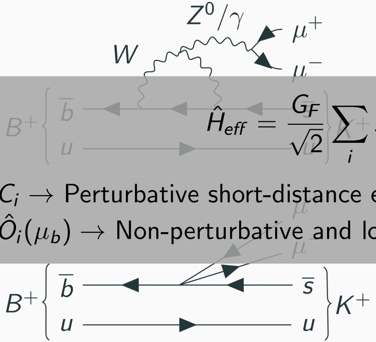

$$\hat{H}_{eff} = \frac{G_F}{\sqrt{2}} \sum_i \lambda_{CKM} C_i \hat{O}_i(\mu_b)$$

$C_i \rightarrow$ Perturbative short-distance effects at energy scale μ_b.

$\hat{O}_i(\mu_b) \rightarrow$ Non-perturbative and long-distance effects.

- In the Effective Field Theory (EFT), the heavy physics ($> M_W$) is integrated out.
- The Wilson coefficients contain all information about short-distance physics.

The b $\to$ sll Anomaly

$$R_{K^{(*)}} = \frac{\mathcal{B}(B \to K^{(*)}\mu^+\mu^-)}{\mathcal{B}(B \to K^{(*)}e^+e^-)}$$

$R_K = 0.846^{+0.060}_{-0.054}(stat.)^{+0.016}_{-0.014}(syst.)$.

- Consistent with SM at **2.5**σ. [1903.09252]

$$R_{K^*} = \begin{cases} 0.66 \,^{+\,0.11}_{-\,0.07}\,(\text{stat}) \pm 0.03\,(\text{syst}) & \text{for } 0.045 < q^2 < 1.1 \ \ \text{GeV}^2/c^4\,, \\ 0.69 \,^{+\,0.11}_{-\,0.07}\,(\text{stat}) \pm 0.05\,(\text{syst}) & \text{for } 1.1 \quad\ < q^2 < 6.0 \ \ \text{GeV}^2/c^4\,. \end{cases}$$

- Consistent with SM at **2.1–2.3**σ and **2.4–2.5**σ respectively. [1705.05802]

The b $\to$ sll Anomaly

$$R_{pK}^{-1} = \frac{\mathcal{B}(\Lambda_b^0 \to pK^+e^+e^-)}{\mathcal{B}(\Lambda_b^0 \to pK^+\mu^+\mu^-)} = 1.17^{+0.18}_{-0.16}(stat.) \pm 0.07(syst.)$$

- Consistent with SM at $\mathbf{1}\sigma$. [1912.08139]

The b $\rightarrow$ sll Anomaly

$$R_{pK}^{-1} = \frac{\mathcal{B}(\Lambda_b^0 \rightarrow pK^+e^+e^-)}{\mathcal{B}(\Lambda_b^0 \rightarrow pK^+\mu^+\mu^-)} = 1.17^{+0.18}_{-0.16}(stat.) \pm 0.07(syst.)$$

- Consistent with SM at $\mathbf{1}\sigma$. [1912.08139]

$B^0 \rightarrow K^*\mu^+\mu^-$ angular mesurements.

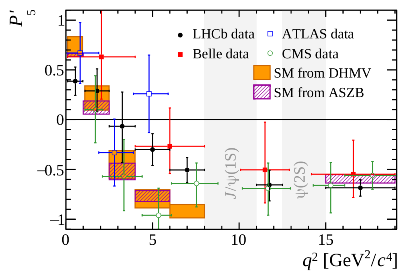

3.4σ tension with the SM. [1512.04442]

The b $\rightarrow$ sll Anomaly

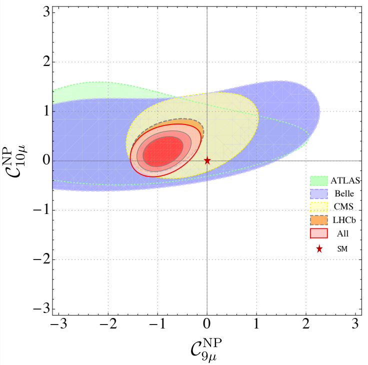

$C_9 \rightarrow$ vector semileptonic coupling.

$C_{10} \rightarrow$ axial-vector semileptonic coupling.

- Global fits to the Wilson coefficients C_9 and C_{10} indicate anomalies in the muon couplings [1903.09578].
- Could be explained by short-distance contributions from NP particles.
- Could also indicate problems in SM predictions for non LFU testing observables.

The short- and long-distance contributions to $B^+ \to K^+\mu^+\mu^-$

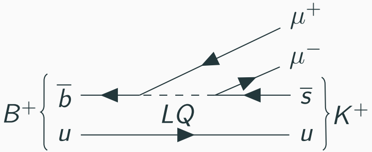

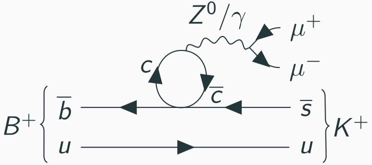

The short- and long-distance contributions to $B^+ \to K^+\mu^+\mu^-$

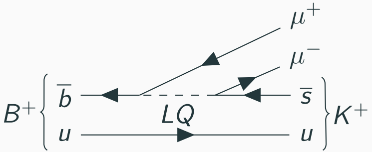

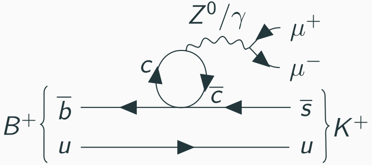

- Recent b $\to$ sll measurements have brought into question calculations of the charm loop contributions.
- Although observation of LFUV would be undeniable sign of NP, in order to determine precisely the couplings involved, these hadronic contributions need to be understood.

Phase difference measurement

$$C_9^{eff} = C_9 + Y(q^2)$$

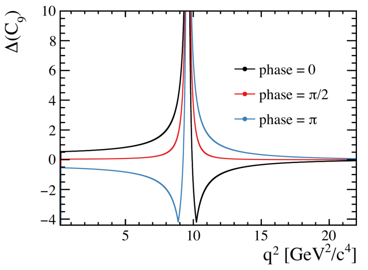

- Non-local contributions could have a large effect in apparent value of C9 depending on the level of the interference.

The phase difference between the resonances and the penguin could account for the anomalies seen in C_9 .

The Complete Analytical Model

The differential decay rate model for $B^+ \to K^+\mu^+\mu^-$ as used in the Run1 analysis is given by,

$$\frac{d\Gamma}{dq^2} = \frac{G_F^2\alpha^2|V_{tb}V_{ts}^*|^2}{2^7\pi^5}|k|\beta\left\{\frac{2}{3}|k|^2\beta^2\left|C_{10}f_+(q^2)\right|^2 + \frac{m_\mu^2(m_B^2-m_K^2)^2}{q^2m_B^2}\left|C_{10}f_0(q^2)\right|^2 \right.$$
$$\left. + |k|^2\left[1-\frac{1}{3}\beta^2\right]\left|C_9^{eff}f_+(q^2)+2C_7\frac{m_b+m_s}{m_B+m_K}f_T(q^2)\right|^2\right\}, \quad (1)$$

[1509.06235]

The Complete Analytical Model

The differential decay rate model for $B^+ \to K^+\mu^+\mu^-$ as used in the Run1 analysis is given by,

$$\frac{d\Gamma}{dq^2} = \frac{G_F^2\alpha^2|V_{tb}V_{ts}^*|^2}{2^7\pi^5}|k|\beta\left\{\frac{2}{3}|k|^2\beta^2\left|C_{10}f_+(q^2)\right|^2 + \frac{m_\mu^2(m_B^2-m_K^2)^2}{q^2m_B^2}\left|C_{10}f_0(q^2)\right|^2\right.$$

$$\left. + |k|^2\left[1-\frac{1}{3}\beta^2\right]\left|C_9^{eff}f_+(q^2) + 2C_7\frac{m_b+m_s}{m_B+m_K}f_T(q^2)\right|^2\right\}, \quad (1)$$

[1509.06235]

$$C_9^{eff} = C_9 + \sum_j \eta_j e^{i\delta_j} A_j^{res}(q^2)$$

η_j is the magnitude and δ_j is the phase. $A^{res}(q^2)$ is a relativistic Breit-Wigner.

- Magnitude and phase of these contributions are allowed to float in the fit along with C_9 , C_{10} and the $f_+(q^2)$ form-factor coefficients.

The Complete Analytical Model

The differential decay rate model for $B^+ \to K^+\mu^+\mu^-$ as used in the Run1 analysis is given by,

$$\frac{d\Gamma}{dq^2} = \frac{G_F^2\alpha^2|V_{tb}V_{ts}^*|^2}{2^7\pi^5}|k|\beta\left\{\frac{2}{3}|k|^2\beta^2\left|C_{10}f_+(q^2)\right|^2 + \frac{m_\mu^2(m_B^2-m_K^2)^2}{q^2m_B^2}\left|C_{10}f_0(q^2)\right|^2\right.$$

$$\left. + |k|^2\left[1-\frac{1}{3}\beta \ldots \right. \ldots)\right|^2 \bigg\} , \quad (1)$$

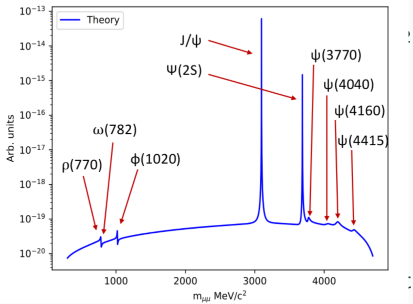

[1509.06235]

η_j is the magnitude a... tivistic Breit-Wigner.

- Magnitude and phase of these contributions are allowed to float in the fit along with C_9 , C_{10} and the $f_+(q^2)$ form-factor coefficients.

Run1 results [1612.06764]

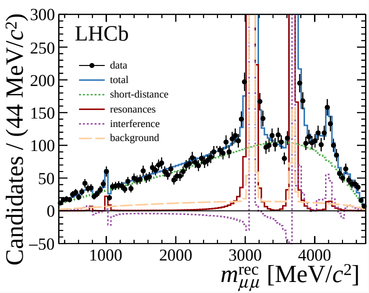

- The precision of J/ψ and $\psi(2S)$ is systematically limited.
- Effect from resonance contributions are small far from their pole.
- Will be interesting to look for additional structures in $m_{\mu\mu}$ around 1770 MeV/c^2

Run1 results [1612.06764]

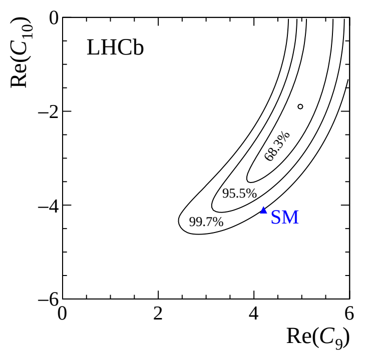

- χ^2 probability intervals with 2 d.o.f.
- The interference with J/ψ does not account for the observed tensions.
- $B \to K$ hadronic form factors are the dominant uncertainty on Wilson's coefficients.

Run1 results [1612.06764]

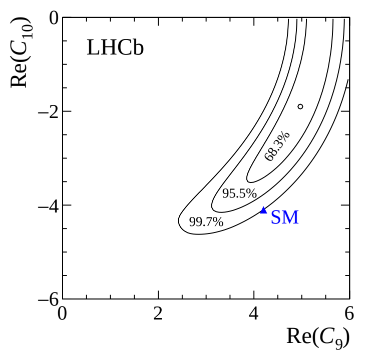

$(C_{9\mu}^{NP}, C_{10\mu}^{NP}) = (\text{-}0.91, 0.18)$

- χ^2 probability intervals with 2 d.o.f.
- The interference with J/ψ does not account for the observed tensions.
- $B \to K$ hadronic form factors are the dominant uncertainty on Wilson's coefficients.

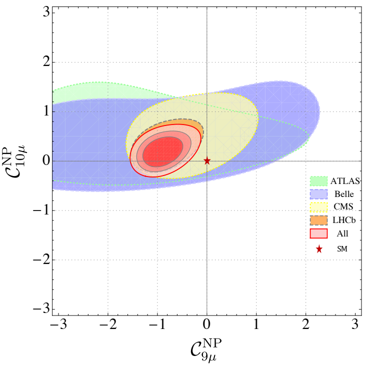

[1903.09578]

Run1 results [1612.06764]

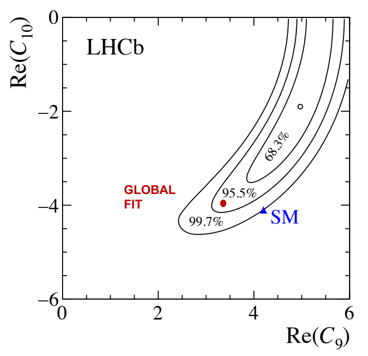

Global fit $(C_{9\mu}, C_{10\mu}) = (3.30, -3.92)$

- More data will help understand this better.
- It will also reduce the hadronic form factor uncertainties.

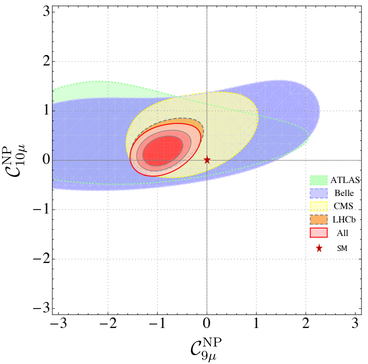

[1903.09578]

Run2 Strategy

- Similar strategy as in Run1 analysis for
  - Detector Resolution,
  - Efficiency Calculation and
  - Treatment of Background
- Expecting to see 5M candidates from Run1 + 2016/17/18 data (Increase in data-set by factor 5).

Run2 Strategy

- Similar strategy as in Run1 analysis for
  - Detector Resolution,
  - Efficiency Calculation and
  - Treatment of Background
- Expecting to see 5M candidates from Run1 + 2016/17/18 data (Increase in data-set by factor 5).
- Moved the analysis framework to TensorFlow for it's in-built CPU parellelization and GPU support.

Run2 Strategy

In addition to accounting for the open-charm resonances as relativistic Breit-Wigners, an alternative method will be implemented.

lakshan.ram@cern.ch

Run2 Strategy

In addition to accounting for the open-charm resonances as relativistic Breit-Wigners, an alternative method will be implemented.

- The charm-loop contribution is calculated through a dispersion relation that uses BESII data on the R-ratio.

$$R(s) = \frac{\sigma(e^+e^- \rightarrow hadrons)}{\sigma(e^+e^- \rightarrow \mu^+\mu^-)}$$

Run2 Strategy

In addition to accounting for the open-charm resonances as relativistic Breit-Wigners, an alternative method will be implemented.

- The charm-loop contribution is calculated through a dispersion relation that uses BESII data on the R-ratio.

$$R(s) = \frac{\sigma(e^+e^- \to hadrons)}{\sigma(e^+e^- \to \mu^+\mu^-)}$$

- The procedure is similar to the one used in Zwicky et al. [1406.0566].
- Separate mag and phase is included for each resonance for the final fit.

Resolution Effects.

Accounting for the detector's resolution effects.

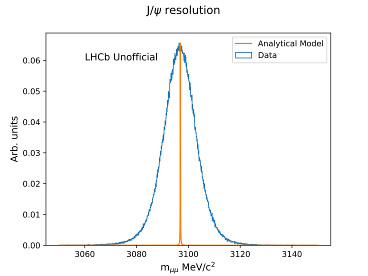

- Improving the resolution is needed to the understand the interference effect.
- When computing $m_{\mu\mu}$, a kinematic fit is performed to the selected candidates. In the fit, the $m_{K\mu\mu}$ mass is constrained to the know B^+ mass to improve the resolution.

Resolution Effects.

- The convolution of the resolution model with the analytical model gives the reconstructed dimuon mass distribution.

$$P(m_{\mu\mu}^{rec}) = R(m_{\mu\mu}^{rec}, m_{\mu\mu}^{true}) \otimes \left[\epsilon(m_{\mu\mu}^{true}) \times 2m_{\mu\mu}^{true} \times \frac{d\Gamma}{dq^2}\right]$$

$\epsilon(m_{\mu\mu}^{true})$ is the detector's efficiency.

Resolution Effects.

- The convolution of the resolution model with the analytical model gives the reconstructed dimuon mass distribution.

$$P(m_{\mu\mu}^{rec}) = R(m_{\mu\mu}^{rec}, m_{\mu\mu}^{true}) \otimes \left[\epsilon(m_{\mu\mu}^{true}) \times 2m_{\mu\mu}^{true} \times \frac{d\Gamma}{dq^2}\right]$$

$\epsilon(m_{\mu\mu}^{true})$ is the detector's efficiency.
Two strategies for the convolution.

- Fast Fourier Transform (FFT) Method
- Performing the convolution integral in steps of $m_{\mu\mu}$

FFT Method

- The dimuon mass distribution is split into three regions and each region is convolved individually with its respective resolution model.
- The convolution is done by TensorFlow's Fast Fourier Transform method.

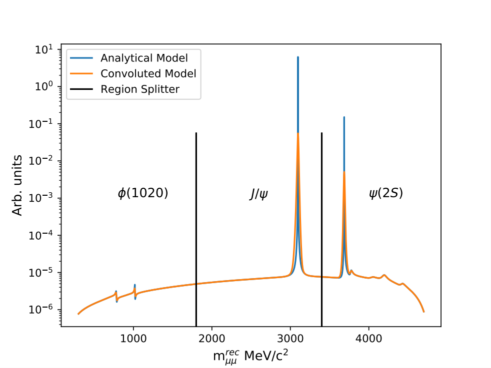

Convolution Integral

The convolution integral is performed in steps of $m_{\mu\mu}^{true}$ using TensorFlow.

$$(f \otimes R)(m_{\mu\mu}^{rec}) = \int_{-\infty}^{\infty} f(m_{\mu\mu}^{true}) R(m_{\mu\mu}^{rec} - m_{\mu\mu}^{true}) dm_{\mu\mu}^{true}$$

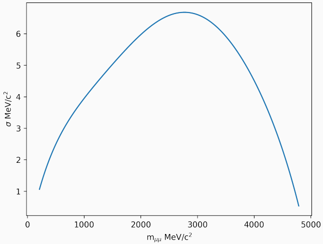

Convolution Integral

The convolution integral is performed in steps of $m_{\mu\mu}^{true}$ using TensorFlow.

$$(f \otimes R)(m_{\mu\mu}^{rec}) = \int_{-\infty}^{\infty} f(m_{\mu\mu}^{true}) R(m_{\mu\mu}^{rec} - m_{\mu\mu}^{true}) dm_{\mu\mu}^{true}$$

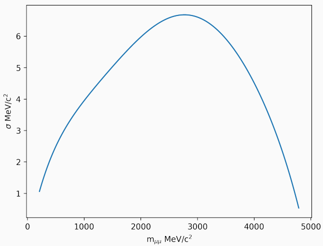

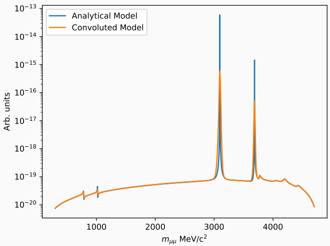

- The latest optimized method still takes about 5 minutes. (An entire fit using the FFT method takes ≈ 3 minutes)
- Currently working on ways to improve the speed.

First look at Run2 data

The J/ψ resonance from 2016/17/18 data.

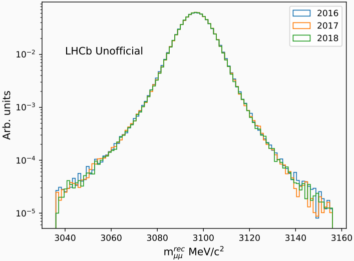

- Given the very good compatibility between the different years, the plan is to merge the data sets together.
- A weighted efficiency using the expected yields will be calculated from the three years.

Run2 Prospects: Precision in Wilson coefficients

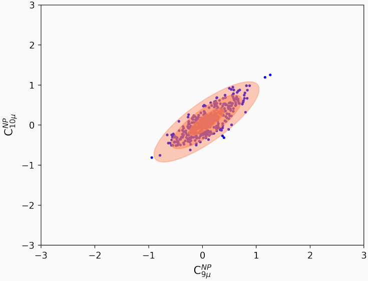

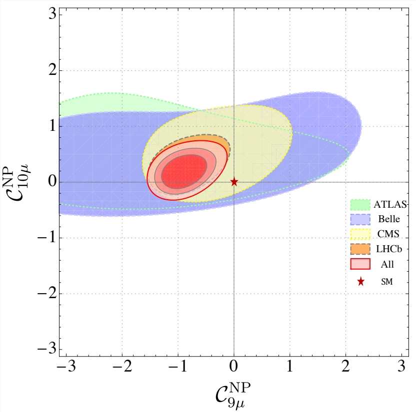

With 5M signal events.

Run1 fit C_9 precision: 10%

Expected C_9 precision: 5%

Run2 Prospects: Form Factor uncertainties.

Form Factor coefficients

Coefficient	Prior [Ref]	Run1 Fit Result	Expected precision (signal only)
b_0^+	0.466 ± 0.014	0.455 ± 0.013	0.465 ± 0.011
b_1^+	-0.89 ± 0.13	-0.78 ± 0.05	-0.889 ± 0.034
b_2^+	-0.21 ± 0.55	0.14 ± 0.33	-0.207 ± 0.212

Gaussian constraints are used in the fit for these coefficients.

$$f_+(q^2) = \frac{1}{1 - /m^2_{B_s^*}} \sum_{i=0}^{N-1} b_i^+ \left[z^i - (-1)^{i-N} \left(\frac{i}{N} \right) z^N \right]$$

With 5M signal events.

Tau loops contribution

Probing b $\rightarrow$ s$\tau\tau$ transitions directly using $B \rightarrow K\tau\tau$ decays is difficult at LHCb due to presence of neutrinos in the final state and lack of information on the B-decay vertex.

Tau loops contribution

Probing b $\to$ s$\tau\tau$ transitions directly using $B \to K\tau\tau$ decays is difficult at LHCb due to presence of neutrinos in the final state and lack of information on the B-decay vertex.

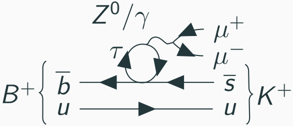

Idea: Search for loop-contributions to the b $\to$ s$\mu\mu$ spectrum.
[Talk by Matthias König]

- Will enter as contributions to C_9^{eff}.
- Large enhancements to tau-couplings C_9^{τ} are motivated by NP explanations to B-anomalies.

Tau loops contribution

Probing b $\to$ s$\tau\tau$ transitions directly using $B \to K\tau\tau$ decays is difficult at LHCb due to presence of neutrinos in the final state and lack of information on the B-decay vertex.

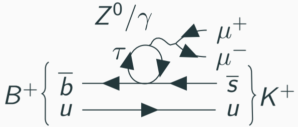

Idea: Search for loop-contributions to the b $\to$ s$\mu\mu$ spectrum.
[Talk by Matthias König]

- Will enter as contributions to C_9^{eff}.
- Large enhancements to tau-couplings C_9^{τ} are motivated by NP explanations to B-anomalies.
- With LHCb's large data set, should be able to see a “cusp” at $m_{\mu\mu} = 2m_{\tau}$.

lakshan.ram@cern.ch

Summary and Outlook

- Need to understand the non-local hadronic loop contributions to quantify NP effects in b $\rightarrow$ sll transitions.
- Will implement alternative models using dispersion relations to describe the charmonium resonances.
- Account for the detector resolution effects using two methods
  - FFT method
  - Convolution Integral
- With the large data set available to LHCb, a search for tau loop contributions will be conducted.

Thank You!

Backup Slides

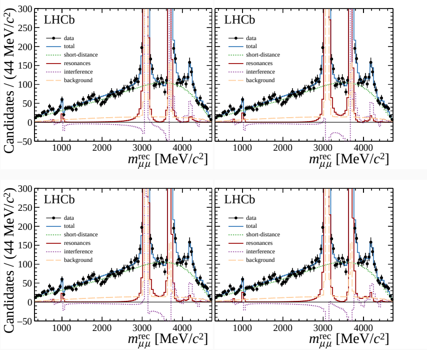

Phase combinations:

- Top Left:
  J/ψ -ve; $\psi(2S)$ -ve
- Top right:
  J/ψ +ve; $\psi(2S)$ -ve
- Bottom Left:
  J/ψ -ve; $\psi(2S)$ +ve
- Bottom Right:
  J/ψ +ve; $\psi(2S)$ +ve

lakshan.ram@cern.ch

Backup Slides

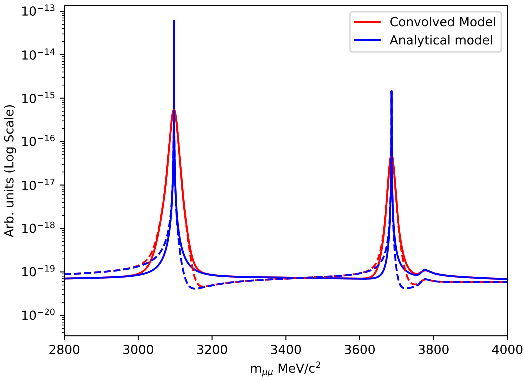

lakshan.ram@cern.ch

Backup Slide - Tau loop cusp

Tau effects in the spectrum

Universität Zürich[UZH]

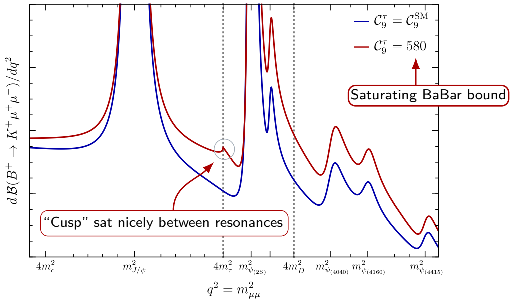

With the amount of data LHCb has, we can find a bound competitive to the current one!

lakshan.ram@cern.ch